Electronic Supplementary Information of

Unusual flexibility of distal and proximal histidine residues in the haem pocket of *Drosophila melanogaster* haemoglobin

Anda Iulia Ioanitescu[a], Sabine Van Doorslaer[a,*], Sylvia Dewilde[b], Luc Moens[b]

[a] Departments of Physics and [b] Biomedical Sciences, University of Antwerp, Universiteitsplein 1, B-2610 Wilrijk-Antwerp, Belgium

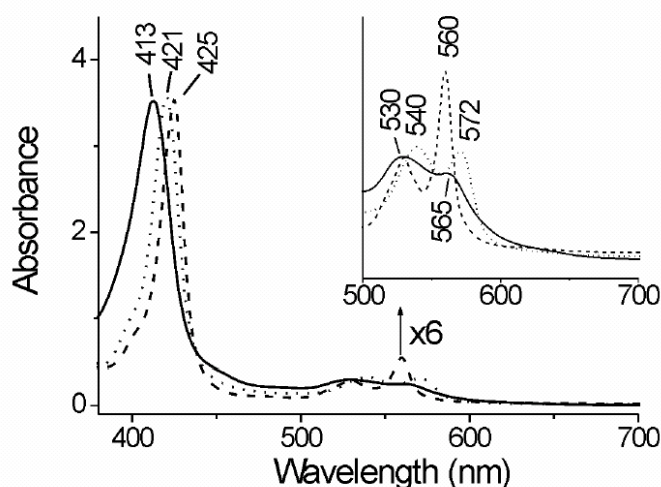UV/Vis absorption spectra of different *Dm*Hb1* forms

Figure S1. Absorption spectra of the [121]Cys → Ser mutant of *Dm*Hb1 (*Dm*Hb1*). The ferric, ferrous deoxy and CO-ligated ferrous forms are represented by solid, dashed and dotted lines, respectively. All proteins were dissolved in 5 mM Tris-HCl buffer at pH 8.5.

The optical spectrum of *Dm*Hb1* in its as-purified form exhibits absorbance maxima at 413, 530 and 565 nm, typical for a ferric low-spin form of the protein (Figure S1, solid line). A small peak at 630 nm is indicative of a high-spin ferric form of *Dm*Hb1* (penta-coordinated ferric or aquomet form), although this might not be the native form of the protein, since protein instability and an open haem pocket have been observed for *Dm*Hb1 [de Sanctis *et al.*, 2005].

The UV-Vis spectrum of the deoxy ferrous form of *Dm*Hb1* obtained after addition of sodium dithionite exhibits the Soret band at 425 nm and the β and α band at 530 and 560 nm respectively (Figure S1, dashed line). This is typical of a hexa-coordinated low-spin ferrous state of the protein. The absorption spectrum of the CO-ligated complex of ferrous *Dm*Hb1* at pH 8.5 shows the Soret band at 421 nm and the α and β bands at respectively 572 and 540 nm, typical for this ligation type (Figure S1, dotted line).

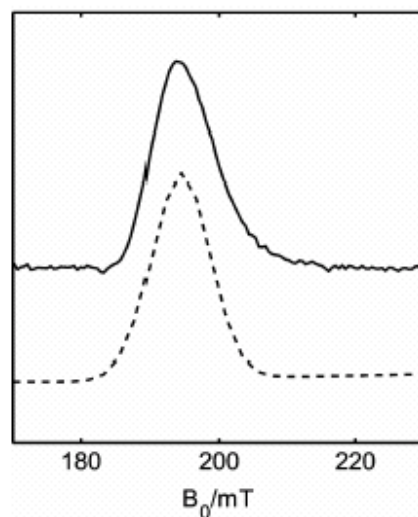CW-EPR spectrum of cyanide-ligated ferric DmHb1*

Figure S2. Experimental (solid line) and simulated (dashed line) CW-EPR spectrum of the cyanide-ligated ferric form of DmHb1*. Only the low-field feature is visible. The spectrum was recorded at 10K. Microwave frequency was 9.4355 GHz.

<u>Comparison with the wild-type *Dm*Hb1</u>

In order to rule out that the different observed components in the CW-EPR spectrum of ferric DmHb1* stem from the mutation, a CW-EPR spectrum of a frozen solution of ferric wild-type *Dm*Hb1 was taken (Figure S3). We see also the appearance of the different LS forms. The wild-type *Dm*Hb1 was obtained as the holoprotein using the method outlined in reference 6 (main text). The current experiment therefore rules out that the observation of different LS forms may be linked to the reconstitution of the protein (insertion of hemin in the apoprotein after isolation) as used for *Dm*Hb1*.
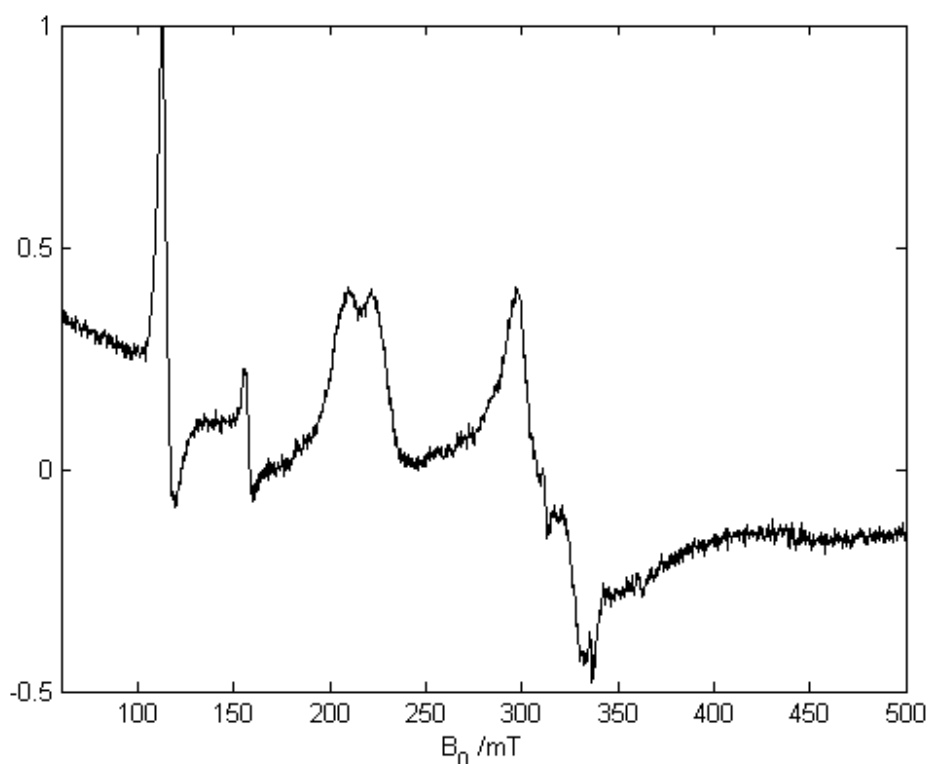

Figure S3. X-band CW-EPR spectrum of ferric wild-type *Dm*Hb1 (frozen solution at pH 8.5, 10 K).

Overlaying experimental and simulated CW-EPR spectra

In the following three figures, the experimental X-band CW-EPR spectra are overlain with the simulations. The simulation parameters are given in Table S1.
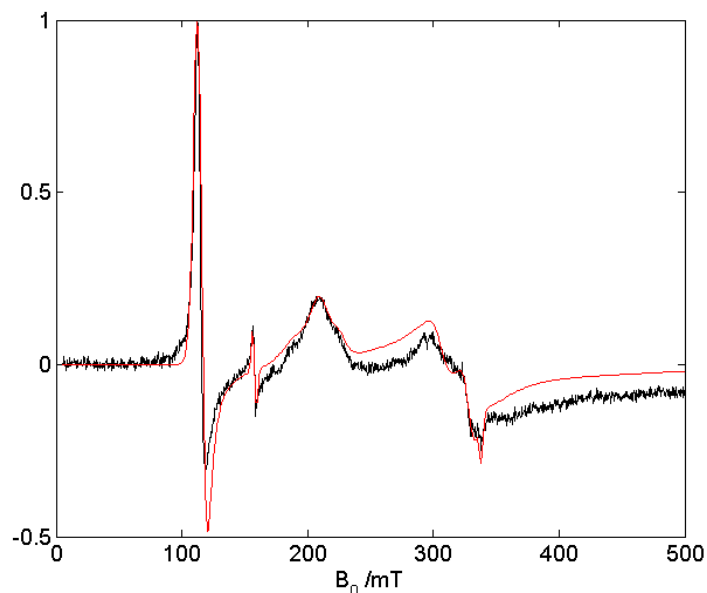
Figure S4a. X-band CW-EPR spectrum of ferric *Dm*Hb1* at pH 5.8 (black: experiment; red: simulation).
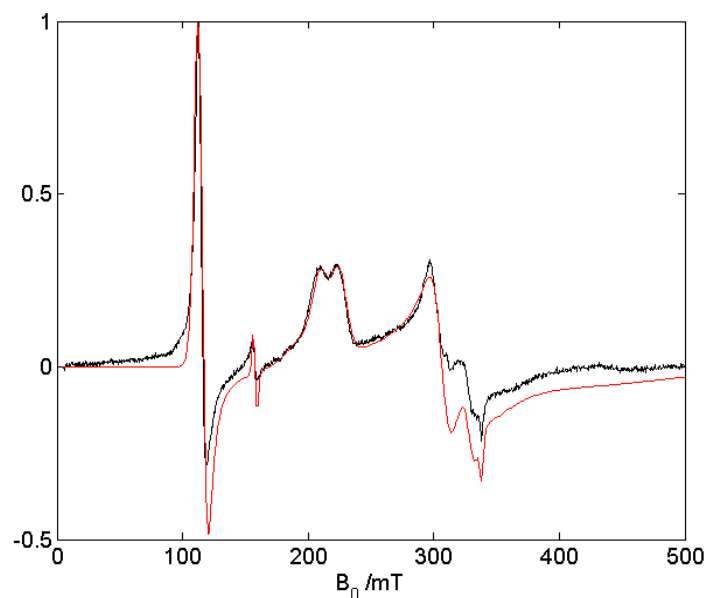
Figure S4b. X-band CW-EPR spectrum of ferric *Dm*Hb1* at pH 8.5 (black: experiment; red: simulation).
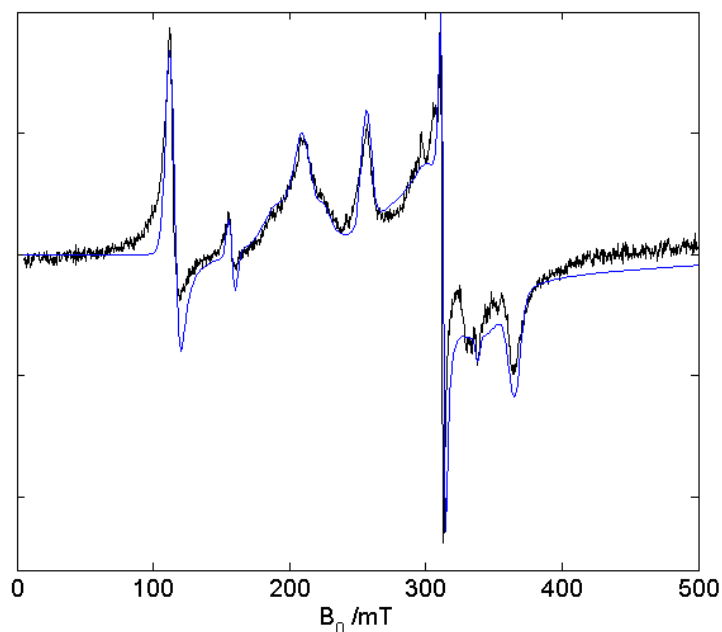
Figure S4 c. X-band CW-EPR spectrum of ferric *Dm*Hb1* at pH 10 (black: experiment; blue: simulation).

Table S1. Simulation parameters used for the simulations of the CW-EPR spectra in Figure S4. l.w. is linewidth given in MHz

	g_z	g_y	g_x	$(l.w.)_z$	$(l.w.)_y$	$(l.w.)_x$
LS1	3.178	2.07	1.25	580	1400	4000
LS2	2.988	2.19	1.5	580	400	2000
LS3	3.50	2.05	0.4	850	850	4000
LS4	2.630	2.155	1.845	305	80	250
HS	5.92	5.88	1.993	850	550	60
Extrahaem iron signal	4.27	4.27	4.27	150	150	150

Note, the lowest g values of LS1, LS2 and LS3 were determined assuming the sum of the squares of the principal *g* values is 16. This is a very rough approximation. The g_x value is found to have only little influence on the spectral part in the [0-400 mT] region for these three LS forms.

Determining the relative spectral contributions of the different components in the CW-EPR spectra

Using the procedure outlined by Svitunenko *et al.* (ref. 26 in main text), a rough estimate of the relative spectral contributions of the different ferric haem forms in *Dm*Hb1* was obtained based on the spectral simulations given in the previous section. We want to stress that, given the fact that the high-field part of LS1-LS3 is not resolved, the values in Table S2 should be considered as indicative rather than quantitative. Especially the values for LS3, for which also the g_y value could not be determined accurately, will have a large error.

Table S2. Estimate of the relative contributions of different ferric haem forms to the CW-EPR spectra of *Dm*Hb1*. Error: 5%

	pH 5.8 (%)	pH 8.5 (%)	pH 10 (%)
LS1	47	44	42
LS2	9	26	8
LS3	16	9	15
LS4	0	0	26
HS	28	21	9

pH dependence of the ESE-detected EPR spectra

As is evident from Figure S5, the ESE-detected EPR spectra of ferric *Dm*Hb1* at pH 10 and pH 8.5 differ quasi only in the LS4 component, whereby the CW-EPR spectra clearly predict a different ratio of LS1/LS2/LS3 for the two pH values (Figure 3). This indicates that the ESE-detected EPR spectra are strongly dominated by the LS2 form, because of the fast phase-memory time of the two other forms. Note that, since the two samples had a different protein concentration, the cavity background signal is not cancelled out when the normalized spectra are subtracted (Figure S5d).

Note that the HS fraction is not observed in the ESE-detected EPR spectra. In order to observe this contribution, the microwave pulses need to be tuned differently and the temperature needs to be lower.
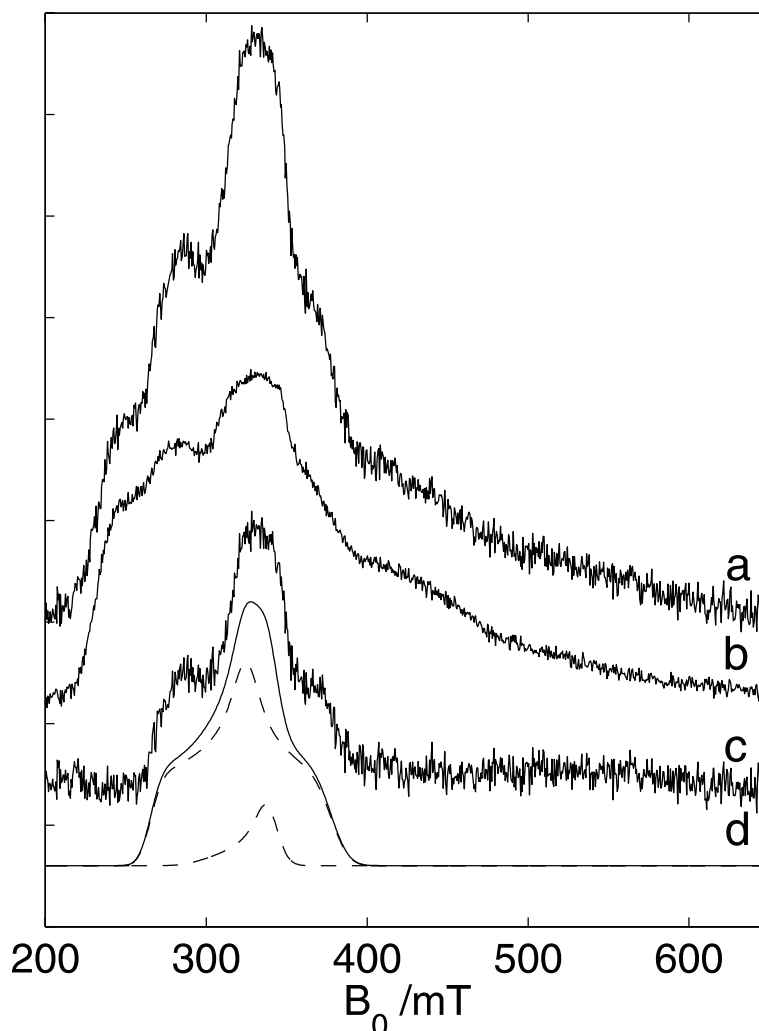
Figure S5. ESE-detected EPR spectrum (τ=112 ns) of ferric *Dm*Hb1* at pH 10 (a) and pH 8.5 (b). The spectra were normalized to the signal at B_0=450 mT. (c) Difference spectrum of (a) − (b). (d) Simulation of (c) as the sum (bold line) of the LS4 contribution and the cavity background signal (both contributions indicated with dashed lines).

Detailed HYSCORE analysis

In the first series, the experimental ^{14}N HYSCORE spectra (black) are overlain with the simulations (red) computed using a three-spin system (S=1/2, $I_{1,2}$=1), whereby the interactions of the unpaired electron between two adjacent haem nitrogens are considered (parameters − Table 2, main text). It is shown that the contributions of these pyrrole nitrogens dominates the nitrogen HYSCORE spectra. In the low-field cases (216.7 and 230.7 mT), additional strong cross peaks linking the nitrogen and proton nuclear frequencies are observed in the (+,+) quadrant.
Comparison of the experimental ^{14}N HYSCORE spectra taken at 216.7 mT (observer position where mainly LS1 and LS3 contribute) and 230.7 mT (observer position agreeing with g=g_z for LS2) reveals no new peaks that can be assigned only to LS1/LS3. All differences can be explained in terms of the change of the field (and consequent change of the nuclear Zeeman frequency).

In the second series, the HYSCORE simulations using the four-spin system (S=1/2, $I_{1,2,3}$=1) are given, whereby the interactions of the unpaired electron with one His nucleus, besides the two haem nitrogens are taken into account. The simulations were done assuming ideal pulses. In principle, real pulses should be assumed and the full spin system (involving all ^{14}N and ^{1}H contributions) should be used to reproduce the exact peak intensities. This would lead to unrealistic simulation times and hence we restrict ourselves to the above system. This restriction limits the accuracy that can be obtained from the simulation (see experimental errors). Also, the high-field HYSCORE spectra are very bad quality, showing only the dq cross peak contributions of the pyrrole nitrogens.

FIRST SERIES: Three-spin system – pyrrole nitrogen contributions
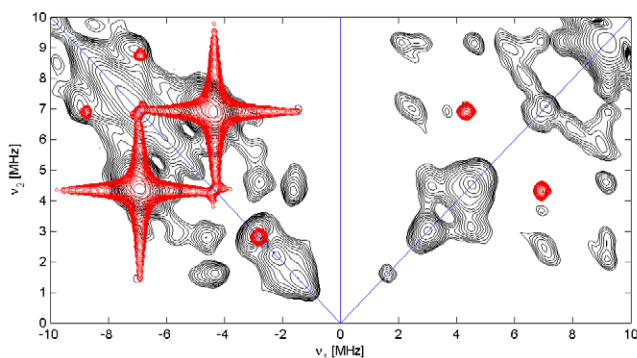
B_0=216.7 mT ((**Figure S6.** (black) ^{14}N HYSCORE spectrum taken at low-field observer position where both LS1 and LS3 are dominantly contributing. (red) Simulation using three-spin system).
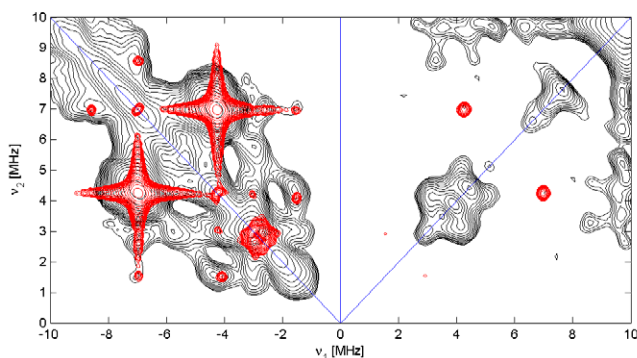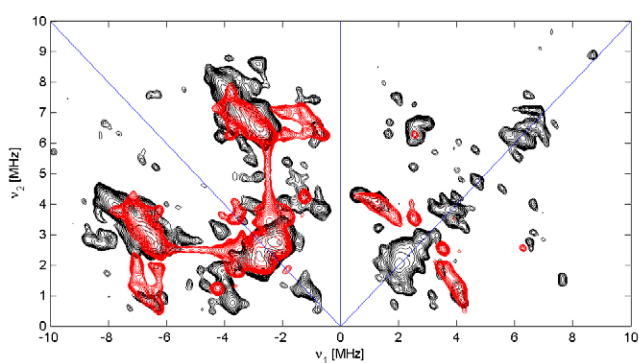

B_0=230.7 mT (**Figure S7.** (black) ^{14}N HYSCORE spectrum taken at low-field observer position where LS2 is dominantly contributing. (red) Simulation using three-spin system).)
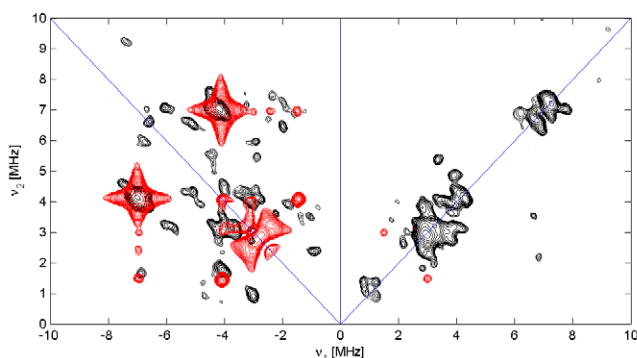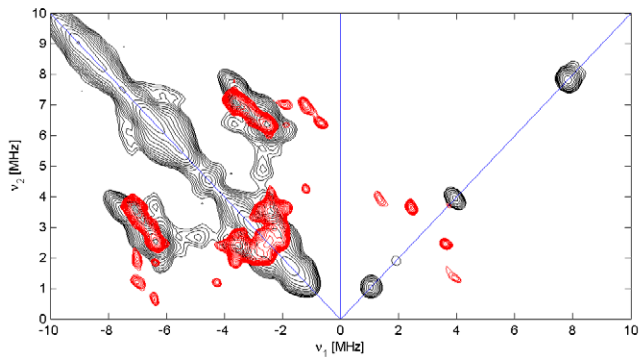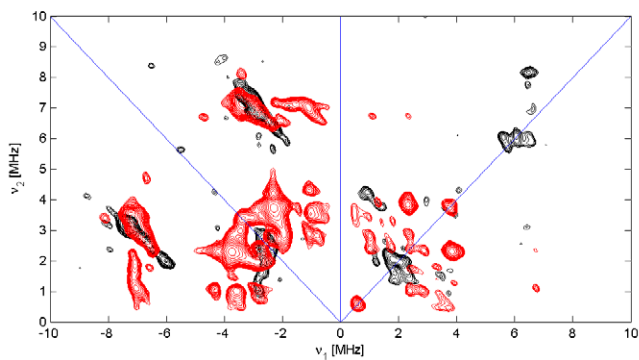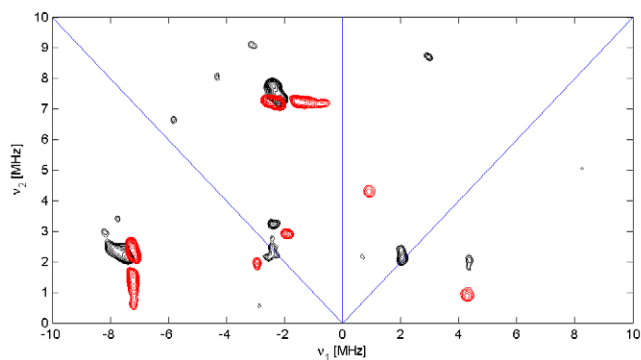

B_0=250 mT
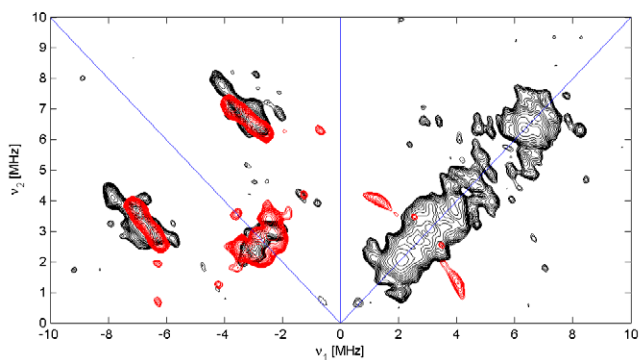
B_0=316.4 mT

B_0=324.1 mT

B_0=337.4 mT

B_0=370.0 mT

B_0=470.0 mT

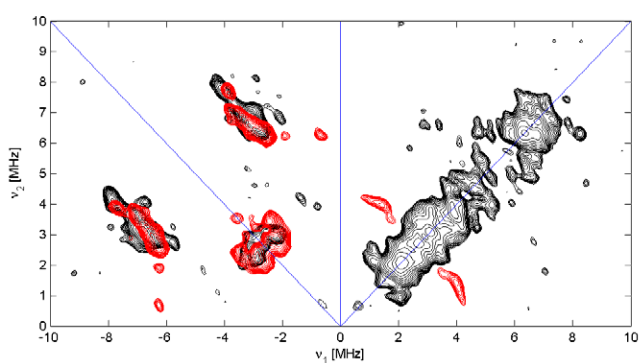SECOND SERIES: Four-spin system – pyrrole + histidine nitrogen contributions
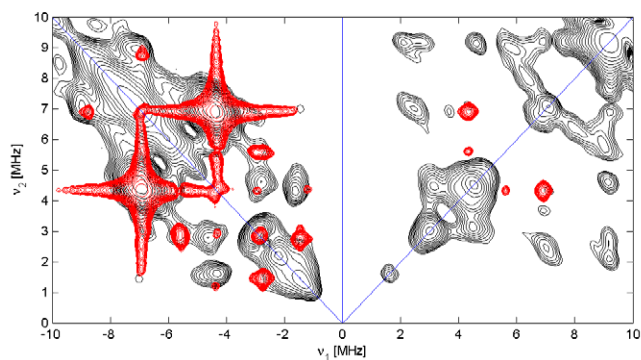
B_0=216.7 mT
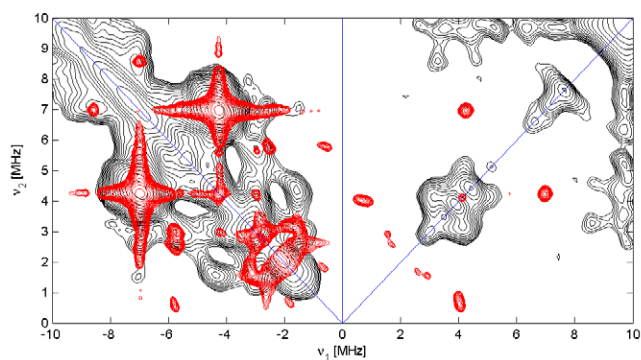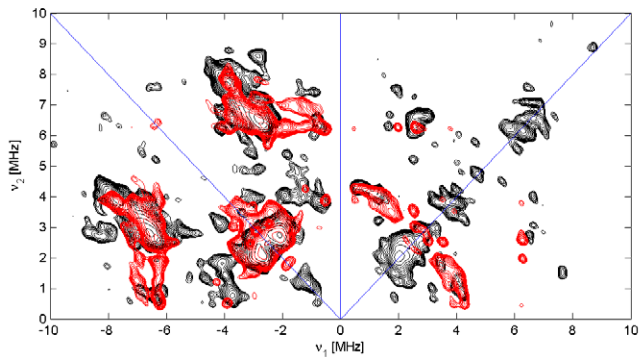

B_0=230.7 mT
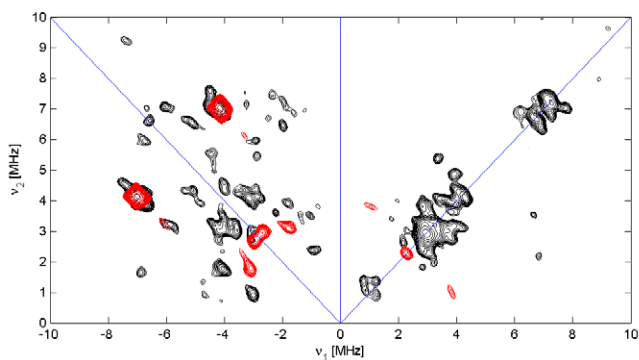
B_0=250.0 mT

B_0=316.4 mT
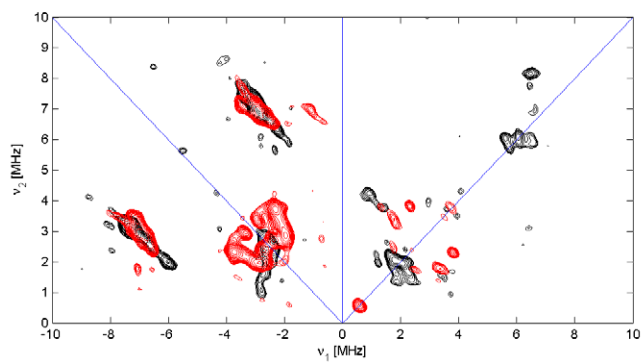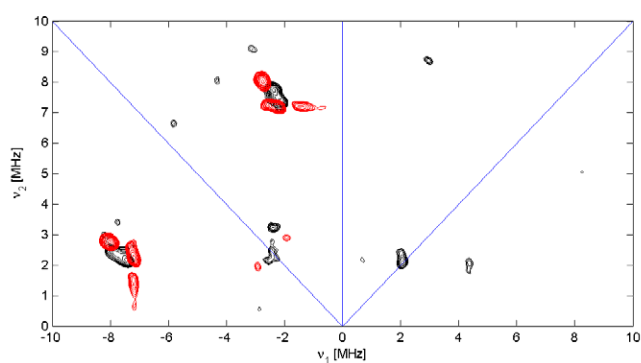

B_0=324.1 mT
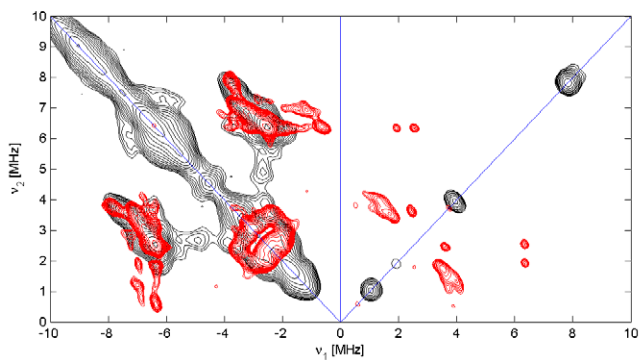
B_0=337.4 mT

B_0=370.0 mT

B_0=470.0 mT

<div align="center">Proton HYSCORE spectra</div>

The proton HYSCORE spectra could only be detected with good accuracy for some of the low-field observer positions. Hence, the proton signals could not be used to determine accurately position of the nearest histidine protons (and hence the relative orientation of the His planes in the *g* tensor frame). Here, we therefore only checked whether the available data can match a dihedral angle of the His planes in the range of 20-40°. The simulations take two sets of nearest protons into account (corresponding to the two His). Furthermore, the matrix protons (peak at (ν_H,ν_H)) is also taken into account. The spectra can be simulated in this way, but insufficient data is available to proof these values unambiguously.
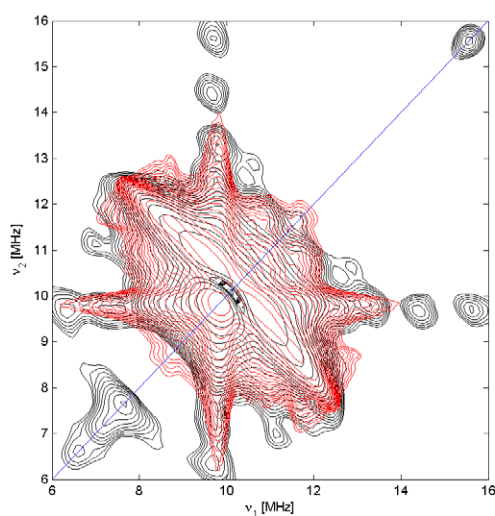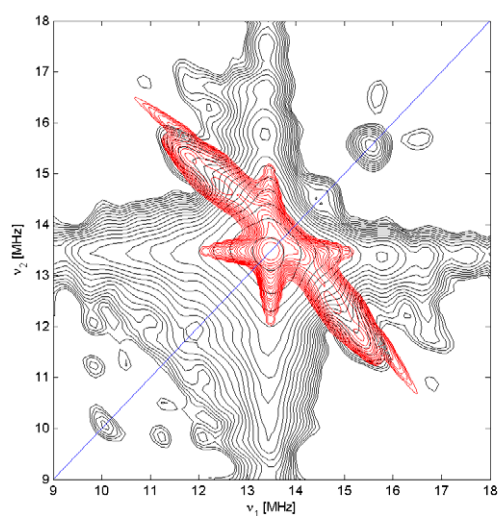
B_0=230.7 mT B_0=316.4 mT

Simulation parameters:
Nearest His protons: ^{1}H(His1): A=[-2.7 -4.8 7.3]±0.5 MHz, α=20°±15°, β=43°±5°, γ=40°±25°
^{1}H(His2): A=[-2.7 -4.8 7.3]±0.5 MHz, α=-15°±15°, β=43°±5°, γ=40°±25°
Matrix protons: ^{1}H: A=[-0.1 –0.1 0.2] ±0.2 MHz